

Generation of Strong Fields to Study the Phase Transitions of Magnetized Warm Dense Matter

 I. N. Erez,^{1,2}  J. R. Davies,²  J. L. Peebles,²  R. Betti,² and  P.-A. Gourdain^{1,2}

¹*Extreme State Physics Laboratory, Physics and Astronomy Department, University of Rochester, Rochester, New York 14627, USA*

²*Laboratory for Laser Energetics, University of Rochester, 250 E. River Road, Rochester, New York 14623, USA*

(*Electronic mail: ierez@lle.rochester.edu)

(Dated: 19 January 2024)

Warm dense matter is a regime where Fermi degenerate electrons take an important role in the macroscopic properties of a material. While recent experiments hinged us closer to better understanding the unmagnetized processes in such dense materials, their magnetized counterpart has been more difficult to study since kilo-Tesla order magnetic fields are required. Although there are examples of field compression generating such fields by compressing pre-magnetized targets, this approach uses a closed configuration, where a converging liner compresses the magnetic flux dynamically. The plasma produced to compress the field is so dense that the fast-heating laser beam required to form warm dense matter cannot penetrate where the field is the highest. In this paper, numerical simulations are used to show that magnetic field compression is also possible by shining the laser beams onto the inner surface of the target, rather than on the outer surface. This approach relies on field compression done by a low-density high-temperature plasma, rather than a high-density low-temperature plasma, used in the more conventional approach. With this novel configuration, the region of the large magnetic field is now mostly free of plasma so the heating beam can reach the sample, located where the magnetic field is the strongest.

I. INTRODUCTION

Warm dense matter (WDM) is defined as strongly-coupled plasma¹ with temperatures in the eV range and densities above solid density². Although the term WDM was first coined by Andrew Ng in 2000³, the studies on it date back to the 1980s¹. WDM is an unexplored state of matter lying in between condensed matter and plasma regimes². Therefore, it is not only relevant to understanding this regime, but it is also key to cutting-edge research done in fusion science⁴ and to a diverse group of astrophysical objects including exoplanets and white dwarfs⁵⁻⁹. At that regime, Fermi degenerate electrons take an important role in the macroscopic properties of a material. Regarding the transitions from solid densities to high energy density plasmas commonly seen in fusion experiments⁴, the understanding of WDM is key to carrying that research forward.

For the theoretical side of the work, there are examples of ab-initio simulations involving Path Integral Monte Carlo (PIMC) methods¹⁰⁻¹³ but experiments are necessary to have a comprehensive validation of such models. Respecting how extreme of a state of matter the WDM is, it is not a trivial task to have it created in a lab environment. One common way to reach these high-energy densities is to use lasers. Ultrafast laser-induced microexplosions confined inside a sapphire can be used for tabletop studies of WDM¹⁴. Intense soft X-ray photoionization is another way to create WDM in a lab environment¹⁵. Not only the creation of WDM in a lab environment is non-trivial, but also probing it is an important task that methods like inelastic X-ray scattering measurements¹⁶ are utilized.

Using diamond-anvil-cells (DACs) and shock-wave experiments, the equation of state (EOS) of materials, partic-

ularly aluminum has been studied¹⁷. While the basic properties of WDM are being explored actively, there is little research devoted to magnetized WDM. For instance, while phase transitions like melting curves are available for various metals^{18,19}, there is no such data for these transitions in the presence of a magnetic field. Therefore, another relevant question both of interest to fusion and astrophysics is: How do phase transitions change under strong magnetic fields? This question is not only fundamental, but also helpful for how to achieve fusion²⁰⁻²⁴, and to obtain better descriptions for astrophysics^{1,25}. Magnetization is promising to be the way to achieve fusion in a lab environment and understanding the behavior of various materials under magnetization is key to solving the fusion problem. MagLIF²⁶ has demonstrated higher yields taking advantage of magnetization of the targets²⁷. Similar behavior is seen in mini MagLIF²⁸ at OMEGA which is a smaller version of MagLIF designed to benefit from high repetition rate experiments. However, due to technical limitations magnetized WDM cannot be explored experimentally.

One main question waiting to be answered in this regime is how a phase transition takes place when degenerate electrons are magnetized. The significant effort happening in the theory community²⁹⁻³³ needs corresponding experiments to be verified. Yet, measuring the phase transition under large electron magnetization is challenging. First, the field must be compressed to reach strengths capable of magnetizing the highly collisional electrons. To estimate the minimum magnetic field required for that, the electron collisional frequency in WDM $\nu_{col,WDM}$ ³⁴ should be compared to the electron cyclotron fre-

quency ω_{ce} . For $v_{col,WDM}$ ³⁴, one can write:

$$v_{col,WDM}(T_e, \omega) \simeq 2\sqrt{2\pi} \frac{Ze^4 n_e}{m^{1/2} (k_B T_e)^{3/2}} \times \ln \left(1 + \frac{1.32}{\sqrt{2\pi}} \frac{k_B T_e}{(m^{1/2} Ze^2 \bar{\omega})^{2/3}} \right) F(T_e, \hbar\omega) \quad (1)$$

where $F(T_e, \hbar\omega) = \sqrt{\frac{\pi}{2}} \langle \frac{u_{th}}{u} \rangle$ is the Fermi factor³⁴. Using this simplified model, one obtains the minimum magnetic field strength required to magnetize the WDM to be $B_{min} \approx 1$ kT for electron number density $n_e = 10^{30} \text{ m}^{-3}$, electron temperature $T_e = 100 \text{ eV}$, and laser wavelength $\lambda = 1000 \text{ nm}$. Second, the high-power beam required for isochoric heating should reach the sample surrounded by the compression plasma. Finally, the samples must be diagnosed, typically using X-rays, which need to traverse the compression plasma and the sample before being measured. This requires a setup capable of accommodating the flux compression geometry and facilitating field measurements to relate changes in material properties to magnetization.

Kilotesla magnetic fields were reached more than a decade ago, using laser-driven magnetic field compression³⁵. More recent work shows that laser-driven cylindrical implosions can compress initial fields of 5 T to 25 kT for magnetized implosions³⁶. Other research showed that kilotesla magnetic field strengths via laser-driven flux compression were possible in a lab environment^{37,38}. However, the challenge here is producing large magnetic fields while getting the necessary access to create and diagnose WDM while measuring the field. These requirements rule out immediately the most common techniques used by the high energy density plasma community, which relies on cylindrical flux compression to generate large magnetic fields³⁵⁻³⁸. In these setups, the cylindrical compression comes from a high-density plasma converging radially, defacto increasing the field. However, the convergent geometry closes all access to the sample, except axially. Yet if the axial direction is used to heat and diagnose the sample, the magnetic field cannot be measured.

This paper explores how magnetic flux compression can be achieved using a low-density plasma which would facilitate the formation and diagnosis of magnetized WDM. This is accomplished by heating the low-density plasma to reach high pressures. To achieve this we propose a setup involving half a hohlraum³⁹ with an initial axial magnetic field of 50 T where the low-density plasma ablated from the inner surface of the halfraum compresses the magnetic field. This proposed setup would allow the heating beam to reach the sample and create WDM while maximizing x-ray transmission. In the rest of the paper, section II presents the proposed design which will be called "halfraum". Then, the results of the 2-D magnetohydrodynamic simulation in PERSEUS⁴⁰ are shared in section III. The findings are discussed in section IV.

II. DESIGN

Cylindrical implosions with high-power lasers are used routinely to compress magnetic fields^{37,41}, even reaching kilo-

tesla strengths. However, the converging configuration blocks the high field region from direct laser illumination, a necessary requirement to produce WDM, at least along the radial direction. While the axial direction can be used, it then becomes difficult to simultaneously heat the sample, diagnose it, and measure the field using proton radiography⁴². Therefore, the conventional compression approach is less than ideal not only for producing WDM but also for diagnosing it while measuring the field.

In order to allow for the sample to be less affected by the field compression, we propose redirecting the compression beams to the inner surface of the cylinder, in a polar drive arrangement reminiscent of hohlraum, used in fusion experiments at NIF³⁹. The cross-section along the radial plane is shown in Figure 1. Using this setup, magnetic flux can be compressed by the low-density plasma ablated by the polar drive beams while keeping the sample in an environment accessible to the heating beam. However, the sample also needs to be diagnosed, for instance using the Powder X-Ray Diffraction Image Plate (PXRDIP)⁴³, which utilizes x-ray Bragg scattering to track the phase transition of magnetized WDM. Consequently, we opted to employ a semi-hohlraum, subsequently named "halfraum." Hence the halfraum refers to a hohlraum cut along its axial plane forming a cylinder with a D-shaped cross-section. Note that traditionally^{44,45}, a halfraum is a hohlraum cut along the polar plane to form a much shorter hohlraum which is different from the halfraum design presented here.

Figure 1 shows a cross-section of the proposed setup, with the sample located on the cylinder axis. For our purposes, a halfraum of inner radius 1 mm with a thickness of 7.9166668 μm is used here. The setup presented here is optimized for the OMEGA laser but can be rescaled easily to other laser facilities such as NIF or LMJ. The halfraum material is plastic and simulated for carbon with an ionization state of 4 and this ionization state is assumed to stay the same throughout the simulation. An initial, axial magnetic field of 50 T is applied externally using the Magneto-Inertial Fusion Electrical Discharge System (MIFEDS) 2.5⁴⁶. While generating such large fields with MIFEDS has not been reported in the literature, this is mostly because MIFEDS is usually used in conjunction with Helmholtz coils, which allow the compression beams to reach the outer cylinder surface. However, our polar drive arrangement does not require access to the outer cylinder surface. Therefore, the coils can be wrapped close to the halfraum. By bringing the conductors right next to the cylinder, fields on the order of 50 T can be generated in theory as in Figure 2.

Since the PXRDIP needs to be close to the WDM sample, we use a 6-turn solenoid with a D-shaped cross-section, similar to the one of the halfraum. We use a radius of 1.75 mm for the half-solenoid, and its geometry is shown in Figure 2. Note that the solenoid was rendered with some transparency to reveal the magnetic fields within it. The magnetic field lines in the figure are only shown in the volume circumscribed inside the halfraum. The coil has a wire radius of 30 μm , with 0.15 mm spacing between the turns, and a spacing of height 0.6 mm. That is to allow the heating beam to pass through

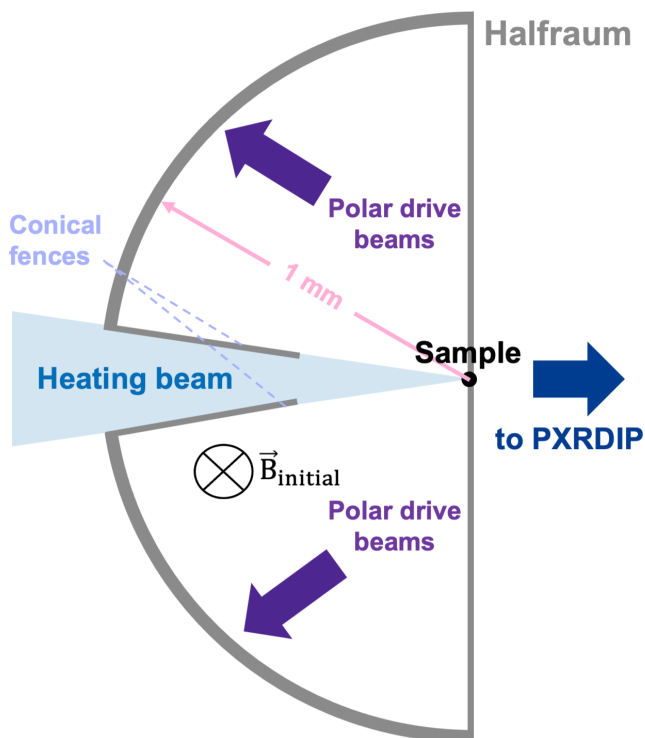


FIG. 1. Polar view of the "halfraum" setup refers to a hohlraum cut along its axial plane to form a D-shaped prism. The half geometry is needed to allow space for the diagnostic hardware of PXRDIP to record the phase transition data. The halfraum is ablated from the inside with polar drive beams to compress the axial magnetic field lines initially applied by MIFEDS 2.5⁴⁶ and to create kilotesla-order magnetization at the sample location. The setup involves a slit with a conical entrance to enable the heating beam to reach the sample for the creation of WDM state.

the slit opening for the conical fence having a base radius of 0.2mm attached to the halfraum. That conical fence is cut at a height of 0.4mm away from the sample as can be seen in Figure 1. For our proposed geometry, the coil inductance comes to 85.9379nH, yielding a peak current of 25kA. Figure 2 is created for that peak current of 25kA which yields the initial magnetic field of 50T within the halfraum.

III. SIMULATION

The novelty of our setup lies in its geometry and the way it allows the introduction of other beams to create and diagnose a WDM sample. The simulations presented in this section ultimately try to answer one main question: Can the design presented here compress the magnetic field to more than 1 kT while allowing the heating beam to penetrate through the ablated plasma to reach the sample for the creation of magnetized WDM? The 2-D MHD code PERSEUS⁴⁷ is used to determine whether experimental conditions can compress fields to a kilotesla, while maintaining a sub-critical density region

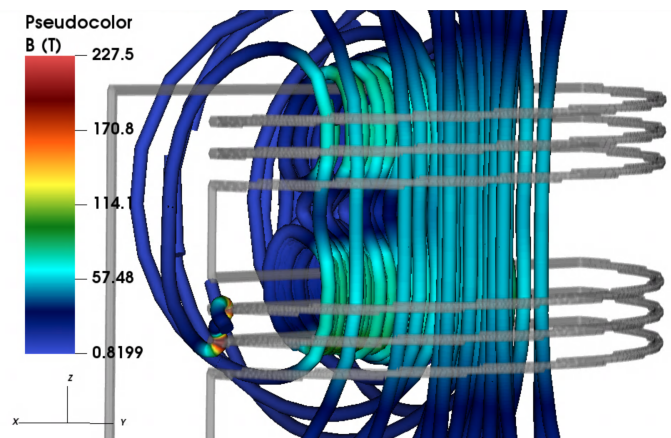


FIG. 2. The coil geometry design introduces the initial axial magnetic field lines using MIFEDS 2.5⁴⁶. The half-solenoid-shaped coil with a radius of 1.75 mm is wrapped around the halfraum. MIFEDS 2.5 can provide a peak current of 25kA to this coil setup of inductance 85.9379nH so that the pictured magnetic fields inside the halfraum can reach the strength 50 T.

in front of the sample. As 2-D MHD simulations do not capture three-dimensional instabilities leading to possibly lower convergence ratios, 3-D models will need to be studied later. One important aspect of the simulations surfaced right away. A complete halfraum would put too much plasma in the heating beam path and a conical fence was attached to the inner surface of the target. Figure 1 shows the cross-section of that conical fence attached to the halfraum target. Note that the conical fence is a slit fence in 2-D.

Our 2-D simulations used a computational domain spanning 2.85 mm with 1.9791667 μm resolution square grids, within a conductive box, necessary to preserve physical boundary conditions on the axial field. Note that the wall of the box has been removed from all the plots. It does not artificially increase the magnetic field at the location of the sample since the box wall is far removed from the sample location and the area ratios at the beginning, and the end of the compression are consistent with the compressed field values. Further, the compression beam and the subsequent laser-plasma interactions are not included in the simulation in this paper. While it is important to estimate their impact on the heating beam, our focus is on how far the electron density is from the critical density. Yet, as should be expected, the electron density along the beam path is found to increase as the slit size decreases, and the field strength at full compression tends to diminish as the slit size increases. A slit size of 0.4mm was sufficient to keep the field strength high while keeping the heating beam path mostly clear of critical density plasma, and the cut for the conical obstacle was similarly kept at a distance of 0.4mm away from the sample location to optimize both density and the field compression. Another simplification inherent to the coil design of Figure 2, is the constant axial field of 50 T throughout the initial simulation domain. We did not model how these magnetic field lines were created in PERSEUS, though the values are consistent with what MIFEDS 2.5 can deliver to the coil as shown in Figure 2.

The simulation is for the first 10 ns after the compression beams hit the halfraum. The laser-plasma interactions here are not simulated, and instead, we provide a power density uniformly distributed on the halfraum's inner surface, corresponding to 20 OMEGA beams, and modeled that as:

$$P_d = Ae^{-\left(\frac{r_{in}-r}{\sigma}\right)^2} \quad (2)$$

where A is a power scaling parameter, and σ is the compression beam penetration depth respectively. $r_{in} = 1$ mm is the inner radius of the halfraum and r is the variable for radius centered at (2.5 mm, 2.1375 mm). σ was set to four grid cells. Note that in the plots, Figure 3 and Figure 4, there is a shift to have the sample at the origin. All the power density is deposited to the halfraum target. The turn-on time is simulated as a 2 ns square pulse with a rise time of 0.1 ns.

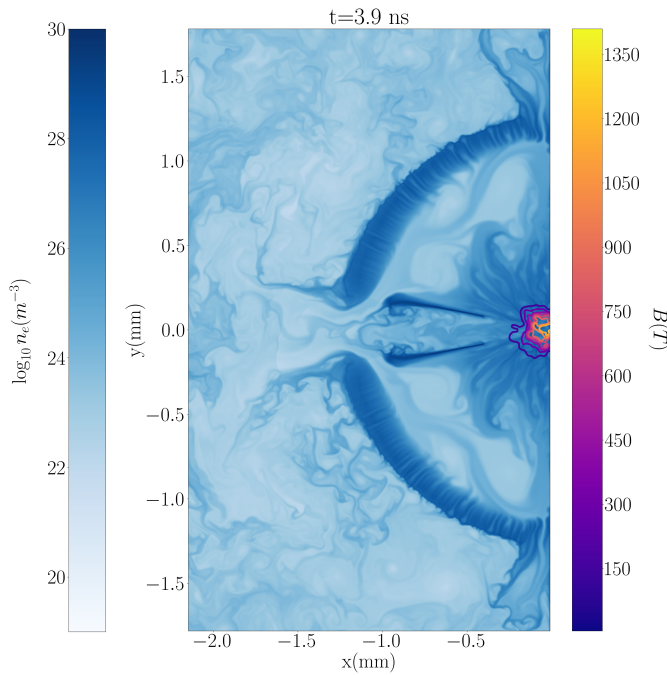


FIG. 3. 3.9 ns after the ablation beam hits the halfraum, the magnetic field strength over 1 kT is reported by PERSEUS simulations at the sample location. One can also see the ablated electrons' behavior and their distributions on this same plot with the log electron density color bar.

The simulation results are shown in Figure 3 and Figure 4 for the time at which $B > 1$ kT is observed along with subcritical densities. Figure 3 shows the contours for the magnetic field strengths superimposed on the ion density, plotted on the logarithmic scale. We see that 3.9 ns after the ablation beam hits the target, the maximum magnetic field strength of 1.3 kT is achieved at the sample location. This can be seen from Figure 3. Note that the boundaries are cropped for the plots reported here and the sample is carried to the origin. For $x < 0$ mm, $y < 0$ mm, and $y > 4.275$ mm, the boundary conditions do not allow the flow of particles implying closed boundaries, while for $x > 2.85$ mm, so on the right side of the

sample, we introduce open boundary conditions in our simulations. This is because the open boundary conditions are more realistic for the boundary around the sample as closed boundary conditions would unrealistically report even higher field strengths with even higher densities due to the trapping of the particles.

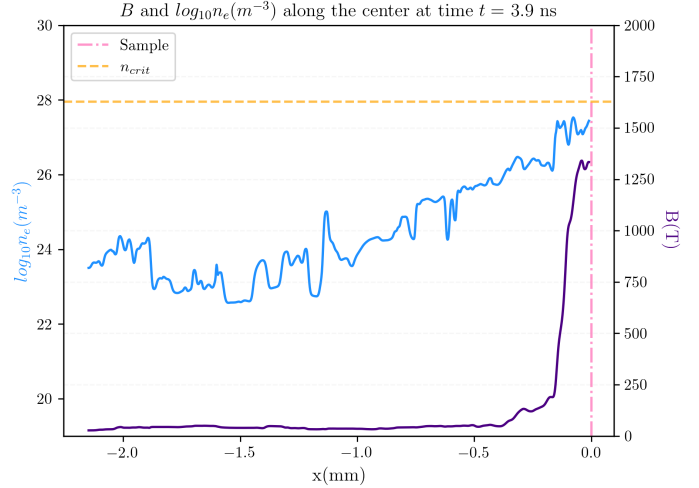


FIG. 4. The lineout plot right along the x-axis shows subcritical electron densities at the peak field region where the sample will be placed. This plot implies that once successful, our setup would enable introducing more beams to create and diagnose magnetized HED matter samples.

Figure 4 shows a lineout taken right at the middle of the y-axis to pass through the slit and the target, and clearly shows that the densities between the target and the slit are below the critical density which is calculated to be $9 \times 10^{27} \text{ m}^{-3}$ for an OMEGA beam of wavelength 351 nm.

IV. DISCUSSION

The results presented here show that the proposed setup allows the generation of fields that can magnetize WDM. However, as in any simulation, there exists room for improvement. One important point is that PERSEUS does not include the Nernst term and having it implemented in our simulations could lead to more realistic results. Yet the temperature gradients and Nernst velocities for the peak field strength indicate that inverting the laser geometry can invert the Nernst velocity as well. The next step would be to have 3-D simulations to better estimate what would be seen in an actual experiment to better investigate possible instabilities.

One possible issue is that the electrons may not be equilibrated at the sample location for the time at which $B > 1$ kT and when the WDM state is created. However, that is not a concern for this work since the simulations do not include the sample and its interaction with the heating beam. The objective is to design an experimental setup, with less emphasis on the specific outcomes that would be obtained from that configuration.

It is demonstrated in this paper that the halfraum setup could potentially be successful in the study of phase transitions in magnetized WDM and open the path to examine magnetized HED matter experimentally. Consequently, the following step would entail the initiation of experiments to further assess the design which should be supported by 3-D simulations.

V. CONCLUSION

In conclusion, an experimental setup for the study of melting curves in a magnetized WDM sample is presented, and its feasibility is demonstrated through 2-D PERSEUS simulations. The design involves a halfraum configuration, created by bisecting a hohlraum along its axis, to enable PXRDIIP diagnostics for precise examination of the phase transition process. In this geometry, the ablated plasma moves inwards, compressing the initially generated magnetic field lines with a strength of 50 T from MIFEDS-2.5, compressed to fields exceeding 1 kT based on our simulations, enabling the magnetization of WDM's valence electrons. Importantly, our simulation results reveal that the plasma density between the sample and the heating beam remains sub-critical, allowing the beam to reach the target. These results show great promise in studying the phase transitions in magnetized WDM, a critical endeavor with significant implications for ongoing research in fusion and astrophysics. The results presented here lead to a novel technique using existing tools to study magnetized HED matter experimentally.

ACKNOWLEDGMENTS

This material is based upon work supported by the Department of Energy [National Nuclear Security Administration] University of Rochester "National Inertial Confinement Fusion Program" under Award Number DE-NA0004144.

This report was prepared as an account of work sponsored by an agency of the U.S. Government. Neither the U.S. Government nor any agency thereof, nor any of their employees, makes any warranty, express or implied, or assumes any legal liability or responsibility for the accuracy, completeness, or usefulness of any information, apparatus, product, or process disclosed, or represents that its use would not infringe privately owned rights. Reference herein to any specific commercial product, process, or service by trade name, trademark, manufacturer, or otherwise does not necessarily constitute or imply its endorsement, recommendation, or favoring by the U.S. Government or any agency thereof. The views and opinions of authors expressed herein do not necessarily state or reflect those of the U.S. Government or any agency thereof.

The research presented here is supported by NSF grant number PHY-2020249 and the Horton fellowship. We acknowledge the members of the Extreme State Physics laboratory at the University of Rochester and the Innovative Concepts Group in the Experimental Division of LLE for their helpful feedback and discussions.

DATA AVAILABILITY STATEMENT

Data available upon request to first author.

Appendix A: Appendixes

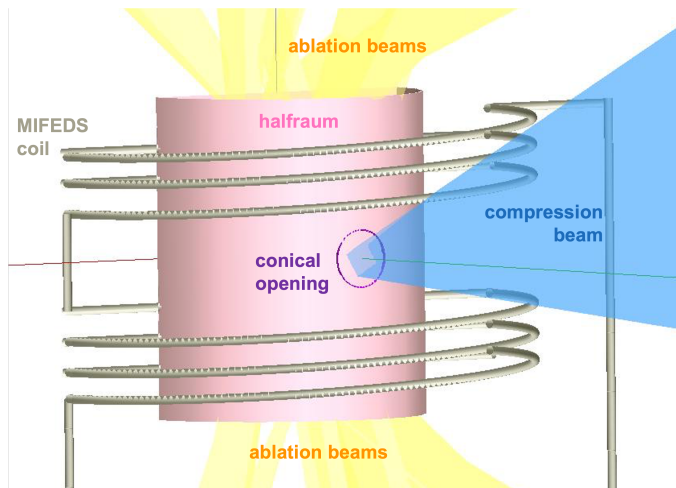


FIG. 5. VisRad model of the setup presented.

- ¹S. Ichimaru, "Strongly coupled plasmas: high-density classical plasmas and degenerate electron liquids," *Rev. Mod. Phys.* **54**, 1017–1059 (1982).
- ²F. R. Graziani, M. P. Desjarlais, R. Redmer, and S. B. Trickey, "Frontiers and challenges in warm dense matter," (2014).
- ³"International workshop on warm dense matter," (May 29–31, 2000).
- ⁴S. B. Hansen, E. C. Harding, P. F. Knapp, M. R. Gomez, T. Nagayama, and J. E. Bailey, "Fluorescence and absorption spectroscopy for warm dense matter studies and icf plasma diagnostics," *Physics of Plasmas* **25**, 056301 (2018), <https://doi.org/10.1063/1.5018580>.
- ⁵M. Koenig, A. Benuzzi-Mounaix, A. Ravasio, T. Vinci, N. Ozaki, S. Lepape, D. Batani, G. Huser, T. Hall, D. Hicks, A. MacKinnon, P. Patel, H. S. Park, T. Boehly, M. Borghesi, S. Kar, and L. Romagnani, "Progress in the study of warm dense matter," *Plasma Physics and Controlled Fusion* **47**, B441 (2005).
- ⁶E. I. Moses, R. N. Boyd, B. A. Remington, C. J. Keane, and R. Al-Ayat, "The national ignition facility: ushering in a new age for high energy density science," *Physics of Plasmas* **16**, 041006 (2009), <https://doi.org/10.1063/1.3116505>.
- ⁷A. Benuzzi-Mounaix, S. Mazevet, A. Ravasio, T. Vinci, A. Denoeud, M. Koenig, N. Amadou, E. Brambrink, F. Festa, A. Levy, M. Harmand, S. Brygoo, G. Huser, V. Recoules, J. Bouchet, G. Morard, F. Guyot, T. de Resseguier, K. Myanishi, N. Ozaki, F. Dorchies, J. Gaudin, P. M. Leguay, O. Peyrusse, O. Henry, D. Raffestin, S. L. Pape, R. Smith, and R. Musella, "Progress in warm dense matter study with applications to planetology," *Physica Scripta* **2014**, 014060 (2014).
- ⁸A. Vailionis, E. G. Gamaly, V. Mizeikis, W. Yang, A. V. Rode, and S. Juodkazis, "Evidence of superdense aluminium synthesized by ultrafast microexplosion," *Nature Communications* **2**, 445 (2011).
- ⁹B. A. Remington, R. M. Cavallo, M. J. Edwards, D. D.-M. Ho, B. F. Lasinski, K. T. Lorenz, H. E. Lorenzana, J. M. Mcnaney, S. M. Pollaine, and R. F. Smith, "Accessing High Pressure States Relevant to Core Conditions in the Giant Planets," *Astrophysics and Space Science* **298**, 235–240 (2005).
- ¹⁰M. Bonitz, T. Dornheim, Z. A. Moldabekov, S. Zhang, P. Hamann, H. Kähler, A. Filinov, K. Ramakrishna, and J. Vorberger, "Ab initio simulation of warm dense matter," *Physics of Plasmas* **27**, 042710 (2020).
- ¹¹T. Dornheim, S. Groth, J. Vorberger, and M. Bonitz, "Ab initio Path Integral Monte Carlo Results for the Dynamic Structure Factor of Correlated

- Electrons: From the Electron Liquid to Warm Dense Matter,” *Physical Review Letters* **121**, 255001 (2018), publisher: American Physical Society.
- ¹²T. Dornheim, S. Groth, and M. Bonitz, “The uniform electron gas at warm dense matter conditions,” *Physics Reports* **744**, 1–86 (2018).
- ¹³P. Hamann, T. Dornheim, J. Vorberger, Z. A. Moldabekov, and M. Bonitz, “Dynamic properties of the warm dense electron gas based on a *b i n i t i o* path integral Monte Carlo simulations,” *Physical Review B* **102**, 125150 (2020).
- ¹⁴A. Vailionis, E. G. Gamaly, V. Mizeikis, W. Yang, A. V. Rode, and S. Juodkazis, “Evidence of superdense aluminium synthesized by ultrafast microexplosion,” *Nature Communications* **2**, 445 (2011), number: 1 Publisher: Nature Publishing Group.
- ¹⁵B. Nagler, U. Zastra, R. R. Faustlin, S. M. Vinko, T. Whitcher, A. J. Nelson, R. Sobierajski, J. Krzywinski, J. Chalupsky, E. Abreu, S. Bajt, T. Bornath, T. Burian, H. Chapman, J. Cihelka, T. Döppner, S. Düsterer, T. Dzelzainis, M. Fajardo, E. Förster, C. Fortmann, E. Galtier, S. H. Glenzer, S. Göde, G. Gregori, V. Hajkova, P. Heimann, L. Juha, M. Jurek, F. Y. Khattak, A. R. Khorsand, D. Klinger, M. Kozlova, T. Laarmann, H. J. Lee, R. W. Lee, K.-H. Meiwes-Broer, P. Mercere, W. J. Murphy, A. Przystawik, R. Redmer, H. Reinholz, D. Riley, G. Röpke, F. Rosmej, K. Saksl, R. Schott, R. Thiele, J. Tiggesbäumker, S. Toleikis, T. Tschentscher, I. Uschmann, H. J. Vollmer, J. S. Wark, and Bob Nagler et al., “Turning solid aluminium transparent by intense soft X-ray photoionization,” *Nature Physics* **5**, 693–696 (2009), number: 9 Publisher: Nature Publishing Group.
- ¹⁶E. García Saiz, G. Gregori, D. O. Gericke, J. Vorberger, B. Barbrel, R. J. Clarke, R. R. Freeman, S. H. Glenzer, F. Y. Khattak, M. Koenig, O. L. Landen, D. Neely, P. Neumayer, M. M. Notley, A. Pelka, D. Price, M. Roth, M. Schollmeier, C. Spindloe, R. L. Weber, L. van Woerkom, K. Wunsch, and D. Riley, “Probing warm dense lithium by inelastic X-ray scattering,” *Nature Physics* **4**, 940–944 (2008), number: 12 Publisher: Nature Publishing Group.
- ¹⁷I. V. Lomonosov, “Multi-phase equation of state for aluminum,” *Laser and Particle Beams* **25**, 567–584 (2007), publisher: Cambridge University Press.
- ¹⁸P. Parisiades, “A Review of the Melting Curves of Transition Metals at High Pressures Using Static Compression Techniques,” *Crystals* **11**, 416 (2021), number: 4 Publisher: Multidisciplinary Digital Publishing Institute.
- ¹⁹O. T. Lord, I. G. Wood, D. P. Dobson, L. Vočadlo, W. Wang, A. R. Thomson, E. T. H. Wann, G. Morard, M. Mezouar, and M. J. Walter, “The melting curve of Ni to 1 Mbar,” *Earth and Planetary Science Letters* **408**, 226–236 (2014).
- ²⁰J. D. Sadler, C. A. Walsh, Y. Zhou, and H. Li, “Role of self-generated magnetic fields in the inertial fusion ignition threshold,” *Physics of Plasmas* **29**, 072701 (2022), <https://doi.org/10.1063/5.0091529>.
- ²¹I. R. Lindemuth, R. E. Reinovsky, R. E. Chrien, J. M. Christian, C. A. Ekdahl, J. H. Goforth, R. C. Haight, G. Idzorek, N. S. King, R. C. Kirkpatrick, R. E. Larson, G. L. Morgan, B. W. Olinger, H. Oona, P. T. Sheehy, J. S. Shlachter, R. C. Smith, L. R. Veese, B. J. Warthen, S. M. Younger, V. K. Chernyshev, V. N. Mokhov, A. N. Demin, Y. N. Dolin, S. F. Garanin, V. A. Ivanov, V. P. Korchagin, O. D. Mikhailov, I. V. Morozov, S. V. Pak, E. S. Pavlovskii, N. Y. Seleznev, A. N. Skobelev, G. I. Volkov, and V. A. Yakubov, “Target plasma formation for magnetic compression/magnetized target fusion,” *Physical Review Letters* **75** (1995), 10.1103/PhysRevLett.75.1953.
- ²²S. A. Slutz, M. C. Herrmann, R. A. Vesey, A. B. Sefkow, D. B. Sinars, D. C. Rovang, K. J. Peterson, and M. E. Cuneo, “Pulsed-power-driven cylindrical liner implosions of laser preheated fuel magnetized with an axial field,” *Physics of Plasmas* **17**, 056303 (2010), <https://doi.org/10.1063/1.3333505>.
- ²³P. F. Knapp, P. F. Schmit, S. B. Hansen, M. R. Gomez, K. D. Hahn, D. B. Sinars, K. J. Peterson, S. A. Slutz, A. B. Sefkow, T. J. Awe, E. Harding, C. A. Jennings, M. P. Desjarlais, G. A. Chandler, G. W. Cooper, M. E. Cuneo, M. Geissel, A. J. Harvey-Thompson, J. L. Porter, G. A. Rochau, D. C. Rovang, C. L. Ruiz, M. E. Savage, I. C. Smith, W. A. Stygar, and M. C. Herrmann, “Effects of magnetization on fusion product trapping and secondary neutron spectra,” *Physics of Plasmas* **22**, 056312 (2015), <https://aip.scitation.org/doi/pdf/10.1063/1.4920948>.
- ²⁴M. E. Cuneo, M. C. Herrmann, D. B. Sinars, S. A. Slutz, W. A. Stygar, R. A. Vesey, A. B. Sefkow, G. A. Rochau, G. A. Chandler, J. E. Bailey, J. L. Porter, R. D. McBride, D. C. Rovang, M. G. Mazarakis, E. P. Yu, D. C. Lamppa, K. J. Peterson, C. Nakhleh, S. B. Hansen, A. J. Lopez, M. E. Savage, C. A. Jennings, M. R. Martin, R. W. Lemke, B. W. Ather-ton, I. C. Smith, P. K. Rambo, M. Jones, M. R. Lopez, P. J. Christenson, M. A. Sweeney, B. Jones, L. A. McPherson, E. Harding, M. R. Gomez, P. F. Knapp, T. J. Awe, R. J. Leeper, C. L. Ruiz, G. W. Cooper, K. D. Hahn, J. McKenney, A. C. Owen, G. R. McKee, G. T. Leifeste, D. J. Ampleford, E. M. Waisman, A. Harvey-Thompson, R. J. Kaye, M. H. Hess, S. E. Rosenthal, and M. K. Matzen, “Magnetically driven implosions for inertial confinement fusion at sandia national laboratories,” *IEEE Transactions on Plasma Science* **40**, 3222–3245 (2012).
- ²⁵B. A. Remington, R. P. Drake, and D. D. Ryutov, “Experimental astrophysics with high power lasers and z pinches,” *Rev. Mod. Phys.* **78**, 755–807 (2006).
- ²⁶S. A. Slutz, M. C. Herrmann, R. A. Vesey, A. B. Sefkow, D. B. Sinars, D. C. Rovang, K. J. Peterson, and M. E. Cuneo, “Pulsed-power-driven cylindrical liner implosions of laser preheated fuel magnetized with an axial field,” *Physics of Plasmas* **17** (2010), 10.1063/1.3333505, eprint: https://pubs.aip.org/aip/pop/article-pdf/doi/10.1063/1.3333505/14920846/056303_1_online.pdf.
- ²⁷M. R. Gomez, S. A. Slutz, A. B. Sefkow, D. B. Sinars, K. D. Hahn, S. B. Hansen, E. C. Harding, P. F. Knapp, P. F. Schmit, C. A. Jennings, T. J. Awe, M. Geissel, D. C. Rovang, G. A. Chandler, G. W. Cooper, M. E. Cuneo, A. J. Harvey-Thompson, M. C. Herrmann, M. H. Hess, O. Johns, D. C. Lamppa, M. R. Martin, R. D. McBride, K. J. Peterson, J. L. Porter, G. K. Robertson, G. A. Rochau, C. L. Ruiz, M. E. Savage, I. C. Smith, W. A. Stygar, and R. A. Vesey, “Experimental demonstration of fusion-relevant conditions in magnetized liner inertial fusion,” *Phys. Rev. Lett.* **113**, 155003 (2014).
- ²⁸J. R. Davies, D. H. Barnak, R. Betti, E. M. Campbell, P.-Y. Chang, A. B. Sefkow, K. J. Peterson, D. B. Sinars, and M. R. Weis, “Laser-driven magnetized liner inertial fusion,” *Physics of Plasmas* **24**, 062701 (2017).
- ²⁹M. Bonitz, T. Dornheim, Z. A. Moldabekov, S. Zhang, P. Hamann, H. Kähler, A. Filinov, K. Ramakrishna, and J. Vorberger, “Ab initio simulation of warm dense matter,” *Physics of Plasmas* **27**, 042710 (2020), <https://doi.org/10.1063/1.5143225>.
- ³⁰D. O. Gericke, K. Wunsch, A. Grinenko, and J. Vorberger, “Structural properties of warm dense matter,” *Journal of Physics: Conference Series* **220**, 012001 (2010).
- ³¹A. Kietzmann, B. Holst, R. Redmer, M. P. Desjarlais, and T. R. Mattsson, “Quantum molecular dynamics simulations for the nonmetal-to-metal transition in fluid helium,” *Phys. Rev. Lett.* **98**, 190602 (2007).
- ³²N. Medvedev and B. Ziaja, “Multistep transition of diamond to warm dense matter state revealed by femtosecond x-ray diffraction,” *Scientific Reports* **8**, 5284 (2018).
- ³³G. M. Petrov, A. Davidson, D. Gordon, and J. Peñano, “Modeling of short-pulse laser-metal interactions in the warm dense matter regime using the two-temperature model,” *Phys. Rev. E* **103**, 033204 (2021).
- ³⁴J. M. ter Vehn, A. Tronnier, and Y. Cang, “Physical collision frequency $v_{eff}(t, \omega)$ for metals and warm dense matter,” in *35th EPS Conference on Plasma Physics 2008 (EPS 2008)*, edited by P. Lalouis (European Physical Society (EPS), 2008).
- ³⁵J. P. Knauer, O. V. Gotchev, P. Y. Chang, D. D. Meyerhofer, O. Polomarov, R. Betti, J. A. Frenje, C. K. Li, M. J.-E. Manuel, R. D. Petrasso, J. R. Rygg, and F. H. Séguin, “Compressing magnetic fields with high-energy lasers,” *Physics of Plasmas* **17**, 056318 (2010), <https://doi.org/10.1063/1.3416557>.
- ³⁶G. Pérez-Callejo, C. Vlachos, C. A. Walsh, R. Florido, M. Bailly-Grandvaux, X. Vaisseau, F. Suzuki-Vidal, C. McGuffey, F. N. Beg, P. Bradford, V. Ospina-Bohórquez, D. Batani, D. Raffestin, A. Colaitis, V. Tikhonchuk, A. Casner, M. Koenig, B. Albertazzi, R. Fedosejevs, N. Woolsey, M. Ehret, A. Debayle, P. Loiseau, A. Calisti, S. Ferri, J. Honrubia, R. Kingham, R. C. Mancini, M. A. Gigosos, and J. J. Santos, “Cylindrical implosion platform for the study of highly magnetized plasmas at laser megajoule,” *Phys. Rev. E* **106**, 035206 (2022).
- ³⁷O. V. Gotchev, P. Y. Chang, J. P. Knauer, D. D. Meyerhofer, O. Polomarov, J. Frenje, C. K. Li, M. J.-E. Manuel, R. D. Petrasso, J. R. Rygg, F. H. Séguin, and R. Betti, “Laser-driven magnetic-flux compression in high-energy-density plasmas,” *Phys. Rev. Lett.* **103**, 215004 (2009).
- ³⁸M. Hohenberger, P.-Y. Chang, G. Fiksel, J. P. Knauer, R. Betti, F. J. Marshall, D. D. Meyerhofer, F. H. Séguin, and R. D. Petrasso, “Inertial confinement fusion implosions with imposed magnetic field compression using the omega laser,” *Physics of Plasmas* **19**, 056306 (2012).

- <https://doi.org/10.1063/1.3696032>.
- ³⁹S. W. Haan, S. M. Pollaine, J. D. Lindl, L. J. Suter, R. L. Berger, L. V. Powers, W. E. Alley, P. A. Amendt, J. A. Futterman, W. K. Levedahl, M. D. Rosen, D. P. Rowley, R. A. Sacks, A. I. Shestakov, G. L. Strobel, M. Tabak, S. V. Weber, G. B. Zimmerman, W. J. Krauser, D. C. Wilson, S. V. Coggeshall, D. B. Harris, N. M. Hoffman, and B. H. Wilde, “Design and modeling of ignition targets for the national ignition facility,” *Physics of Plasmas* **2**, 2480–2487 (1995), <https://doi.org/10.1063/1.871209>.
- ⁴⁰C. E. Seyler and M. R. Martin, “Relaxation model for extended magnetohydrodynamics: Comparison to magnetohydrodynamics for dense z-pinch,” *Physics of Plasmas* **18**, 012703 (2011), <https://doi.org/10.1063/1.3543799>.
- ⁴¹D. Kawahito, M. Bailly-Grandvaux, M. Dozières, C. McGuffey, P. Forestier-Colleoni, J. Peebles, J. J. Honrubia, B. Khiar, S. Hansen, P. Tzeferacos, M. S. Wei, C. M. Krauland, P. Gourdain, J. R. Davies, K. Matsuo, S. Fujioka, E. M. Campbell, J. J. Santos, D. Batani, K. Bhutwala, S. Zhang, and F. N. Beg, “Fast electron transport dynamics and energy deposition in magnetized, imploded cylindrical plasma,” *Philosophical Transactions of the Royal Society A: Mathematical, Physical and Engineering Sciences* **379**, 10.1098/rsta.2020.0052.
- ⁴²A. J. Mackinnon, P. K. Patel, R. P. Town, M. J. Edwards, T. Phillips, S. C. Lerner, D. W. Price, D. Hicks, M. H. Key, S. Hatchett, S. C. Wilks, M. Borghesi, L. Romagnani, S. Kar, T. Toncian, G. Pretzler, O. Willi, M. Koenig, E. Martinoli, S. Lepape, A. Benuzzi-Mounaix, P. Audebert, J. C. Gauthier, J. King, R. Snavely, R. R. Freeman, and T. Boehlly, “Proton radiography as an electromagnetic field and density perturbation diagnostic (invited),” *Review of Scientific Instruments* **75**, 3531–3536 (2004), <https://doi.org/10.1063/1.1788893>.
- ⁴³J. R. Rygg, J. H. Eggert, A. E. Lazicki, F. Coppari, J. A. Hawreliak, D. G. Hicks, R. F. Smith, C. M. Sorce, T. M. Uphaus, B. Yaakobi, and G. W. Collins, “Powder diffraction from solids in the terapascal regime,” *Review of Scientific Instruments* **83**, 113904 (2012), <https://doi.org/10.1063/1.4766464>.
- ⁴⁴S. A. MacLaren, C. A. Back, and J. H. Hammer, “Measurements and calculations of halfraum radiation drives at the omega laser,” *Journal of Quantitative Spectroscopy and Radiative Transfer* **99**, 398–408 (2006), radiative Properties of Hot Dense Matter.
- ⁴⁵H. Johns, C. Fryer, S. Wood, C. Fontes, P. Kozlowski, N. Lanier, A. Liao, T. Perry, J. Morton, C. Brown, D. Schmidt, T. Cardenas, T. Urbatsch, P. Hakel, J. Colgan, S. Coffing, J. Cowan, D. Capelli, L. Goodwin, T. Quintana, C. Hamilton, F. Fierro, C. Wilson, R. Randolph, P. Donovan, T. Sedillo, R. Gonzales, M. Sherrill, M. Douglas, W. Garbett, J. Hager, and J. Kline, “A temperature profile diagnostic for radiation waves on omega-60,” *High Energy Density Physics* **39**, 100939 (2021).
- ⁴⁶O. V. Gotchev, J. P. Knauer, P. Y. Chang, N. W. Jang, M. J. Shoup, D. D. Meyerhofer, and R. Betti, “Seeding magnetic fields for laser-driven flux compression in high-energy-density plasmas,” *Review of Scientific Instruments* **80**, 043504 (2009), <https://doi.org/10.1063/1.3115983>.
- ⁴⁷C. E. Seyler and M. R. Martin, “Relaxation model for extended magnetohydrodynamics: Comparison to magnetohydrodynamics for dense z-pinch,” *Physics of Plasmas* **18**, 012703 (2011), <https://doi.org/10.1063/1.3543799>.
- ⁴⁸A. Lavagno and F. Lingua, “Effects of strong magnetic fields in dense stellar matter,” *Proceedings of the International Astronomical Union* **9**, 439–440 (2013), publisher: Cambridge University Press.
- ⁴⁹A. Rabhi and C. Providência, “Dense stellar matter with trapped neutrinos under strong magnetic fields,” *Journal of Physics G: Nuclear and Particle Physics* **37**, 075102 (2010).
- ⁵⁰A. Rabhi, P. K. Panda, and C. Providência, “Warm and dense stellar matter under strong magnetic fields,” *Physical Review C* **84**, 035803 (2011).
- ⁵¹D. H. Barnak, J. R. Davies, G. Fiksel, P.-Y. Chang, E. Zabir, and R. Betti, “Increasing the magnetic-field capability of the magnetoinertial fusion electrical discharge system using an inductively coupled coil,” *Review of Scientific Instruments* **89**, 033501 (2018), <https://doi.org/10.1063/1.5012531>.
- ⁵²G. Fiksel, A. Agliata, D. Barnak, G. Brent, P.-Y. Chang, L. Folsnbee, G. Gates, D. Hasset, D. Lonobile, J. Magoon, D. Mastro Simone, M. J. Shoup, and R. Betti, “Note: Experimental platform for magnetized high-energy-density plasma studies at the omega laser facility,” *Review of Scientific Instruments* **86**, 016105 (2015), <https://doi.org/10.1063/1.4905625>.
- ⁵³O. V. Gotchev, J. P. Knauer, P. Y. Chang, N. W. Jang, M. J. Shoup, III, D. D. Meyerhofer, and R. Betti, “Seeding magnetic fields for laser-driven flux compression in high-energy-density plasmas,” *Review of Scientific Instruments* **80**, 043504 (2009).
- ⁵⁴J. R. Rygg, J. H. Eggert, A. E. Lazicki, F. Coppari, J. A. Hawreliak, D. G. Hicks, R. F. Smith, C. M. Sorce, T. M. Uphaus, B. Yaakobi, and G. W. Collins, “Powder diffraction from solids in the terapascal regime,” *Review of Scientific Instruments* **83**, 113904 (2012).
- ⁵⁵G. Norman and I. Saitov, “Plasma phase transition in warm dense hydrogen,” *Contributions to Plasma Physics* **58**, 122–127 (2018), <https://onlinelibrary.wiley.com/doi/pdf/10.1002/ctpp.201700101>.
- ⁵⁶D. Kraus, *Characterization of phase transitions in warm dense matter with X-ray scattering*, Ph.D. thesis (2012).
- ⁵⁷M. Murakami, J. J. Honrubia, K. Weichman, A. V. Arefiev, and S. V. Bulanov, “Generation of megatesla magnetic fields by intense-laser-driven microtube implosions,” *Scientific Reports* **10**, 16653 (2020).
- ⁵⁸D. Nakamura, A. Ikeda, H. Sawabe, Y. H. Matsuda, and S. Takeyama, “Record indoor magnetic field of 1200 t generated by electromagnetic flux-compression,” *Review of Scientific Instruments* **89**, 095106 (2018), <https://doi.org/10.1063/1.5044557>.
- ⁵⁹Q. Zeng and J. Dai, “Structural transition dynamics of the formation of warm dense gold: From an atomic scale view,” *Science China Physics, Mechanics & Astronomy* **63**, 263011 (2020).
- ⁶⁰M. Mo, Z. Chen, and S. Glenzer, “Ultrafast visualization of phase transitions in nonequilibrium warm dense matter,” *MRS Bulletin* **46**, 694–703 (2021).
- ⁶¹M. Z. Mo, Z. Chen, R. K. Li, M. Dunning, B. B. L. Witte, J. K. Baldwin, L. B. Fletcher, J. B. Kim, A. Ng, R. Redmer, A. H. Reid, P. Shekhar, X. Z. Shen, M. Shen, K. Sokolowski-Tinten, Y. Y. Tsui, Y. Q. Wang, Q. Zheng, X. J. Wang, and S. H. Glenzer, “Heterogeneous to homogeneous melting transition visualized with ultrafast electron diffraction,” *Science* **360**, 1451–1455 (2018), <https://www.science.org/doi/pdf/10.1126/science.aar2058>.
- ⁶²I. Inoue, Y. Inubushi, T. Sato, K. Tono, T. Katayama, T. Kameshima, K. Ogawa, T. Togashi, S. Owada, Y. Amemiya, T. Tanaka, T. Hara, and M. Yabashi, “Observation of femtosecond X-ray interactions with matter using an X-ray-X-ray pump-probe scheme,” *Proceedings of the National Academy of Science* **113**, 1492–1497 (2016).
- ⁶³A. Pelka, G. Gregori, D. O. Gericke, J. Vorberger, S. H. Glenzer, M. M. Günther, K. Harres, R. Heathcote, A. L. Kritcher, N. L. Kugland, B. Li, M. Makita, J. Mithen, D. Neely, C. Niemann, A. Otten, D. Riley, G. Schauermann, M. Schollmeier, A. Tauschwitz, and M. Roth, “Ultrafast melting of carbon induced by intense proton beams,” *Phys. Rev. Lett.* **105**, 265701 (2010).
- ⁶⁴G. Pérez-Callejo, C. Vlachos, C. A. Walsh, R. Florido, M. Bailly-Grandvaux, X. Vaisseau, F. Suzuki-Vidal, C. McGuffey, F. N. Beg, P. Bradford, V. Ospina-Bohórquez, D. Batani, D. Raffestin, A. Colaitis, V. Tikhonchuk, A. Casner, M. Koenig, B. Albertazzi, R. Fedosejevs, N. Woolsey, M. Ehret, A. Debayle, P. Loiseau, A. Calisti, S. Ferri, J. Honrubia, R. Kingham, R. C. Mancini, M. A. Gigosos, and J. J. Santos, “Cylindrical implosion platform for the study of highly magnetized plasmas at laser megajoule,” *Phys. Rev. E* **106**, 035206 (2022).
- ⁶⁵O. V. Gotchev, P. Y. Chang, J. P. Knauer, D. D. Meyerhofer, O. Polomarov, J. Freije, C. K. Li, M. J.-E. Manuel, R. D. Petrasso, J. R. Rygg, F. H. Séguin, and R. Betti, “Laser-driven magnetic-flux compression in high-energy-density plasmas,” *Phys. Rev. Lett.* **103**, 215004 (2009).